

Small Molecule Inhibitors Of The PCSK9•LDLR Interaction

Jaru Taechalerpaisarn, Bosheng Zhao, Xiaowen Liang, and Kevin Burgess

J. Am. Chem. Soc., **Just Accepted Manuscript** • DOI: 10.1021/jacs.7b09360 • Publication Date (Web): 29 Jan 2018

Downloaded from <http://pubs.acs.org> on January 30, 2018

Just Accepted

“Just Accepted” manuscripts have been peer-reviewed and accepted for publication. They are posted online prior to technical editing, formatting for publication and author proofing. The American Chemical Society provides “Just Accepted” as a free service to the research community to expedite the dissemination of scientific material as soon as possible after acceptance. “Just Accepted” manuscripts appear in full in PDF format accompanied by an HTML abstract. “Just Accepted” manuscripts have been fully peer reviewed, but should not be considered the official version of record. They are accessible to all readers and citable by the Digital Object Identifier (DOI®). “Just Accepted” is an optional service offered to authors. Therefore, the “Just Accepted” Web site may not include all articles that will be published in the journal. After a manuscript is technically edited and formatted, it will be removed from the “Just Accepted” Web site and published as an ASAP article. Note that technical editing may introduce minor changes to the manuscript text and/or graphics which could affect content, and all legal disclaimers and ethical guidelines that apply to the journal pertain. ACS cannot be held responsible for errors or consequences arising from the use of information contained in these “Just Accepted” manuscripts.

Small Molecule Inhibitors Of The PCSK9•LDLR Interaction

Jaru Taechalertpaisarn,¹ Bosheng Zhao,¹ Xiaowen Liang,² and Kevin Burgess*¹

¹ Department of Chemistry, Texas A & M University, Box 30012, College Station, TX 77842,
USA

² Center for Infectious and Inflammatory Diseases, 2121 W. Holcombe Blvd.,
Houston, TX 77030, USA

E-mail: burgess@tamu.edu

RECEIVED DATE

TITLE RUNNING HEAD: Inhibitors of PCSK9•LDLR

ABSTRACT

The protein-protein interaction between proprotein convertase subtilisin/kexin type 9 (PCSK9) and low-density lipoprotein receptor (LDLR) is a relatively new, and extremely important, validated therapeutic target for treatment and prevention of heart disease. Experts in the area agree that the first small molecules to disrupt PCSK9•LDLR would represent a milestone in this field, yet no credible leads have been reported. This paper describes how side-chain orientations in preferred conformations of carefully designed chemotypes were compared with LDLR side-chains at the PCSK9•LDLR interface to find molecules that would mimic interface regions of LDLR. This approach is an example of the procedure called EKO (Exploring Key Orientations). The guiding hypothesis on which EKO is based is that good matches indicate the chemotypes bearing the same side-chains as the protein at the sites of overlay have the potential to disrupt the parent protein-protein interaction (PPI). In the event, the EKO procedure and one round of combinatorial fragment-based virtual docking, led to the discovery of seven compounds that bound PCSK9 (SPR and ELISA) and had a favorable outcome in a cellular assay (hepatocyte uptake of fluorescently labeled LDL particles) and increased the expression LDLR on hepatocytes in culture. Three promising hit compounds in this series had dissociation constants for PCSK9 binding in the 20 – 40 μ M range, and one of these was modified with a photoaffinity label and shown to form a covalent conjugate with PCSK9 on photolysis.

INTRODUCTION

1
2 Heart disease, a leading cause of death, is frequently associated with plaque in the arteries
3
4 causing atherosclerosis, which is attributed by elevated levels of low density lipoprotein (LDL)
5
6 in the blood. LDLRs (LDL-receptors), on the surface of hepatocytes, are responsible for
7
8 capturing LDL particles, and importing them into the liver for destruction. Thus, LDLR•LDL
9
10 complexes on the surface of hepatocytes undergo clathrin-mediated endocytosis into
11
12 endosomes wherein the acidic environment triggers rearrangement of the LDLR extracellular
13
14 domain, releasing bound lipoproteins, leaving the LDLR to be recycled to the plasma
15
16 membrane (Figure 1a).¹
17
18
19
20

21
22 Removal of LDL particles by hepatocytes is negatively modulated by a chaperone called
23
24 PCSK9^{2,3} that recognizes plasma membrane LDLR.⁴ PCSK9 inhibits the rearrangement of
25
26 LDLR in LDLR•LDL complexes, so that *the receptor is not recycled to the plasma membrane*
27
28 *but is instead routed to lysosomes where LDL, LDLR and PCSK9 are degraded* (Figure 1b).⁵⁻⁸
29
30 Plasma LDL cholesterol levels thus can be *decreased* by inhibiting the PCSK9•LDLR
31
32 interaction, because that *increases* the display of LDLR on the hepatocytes.^{1,9,10} This effect
33
34 was discovered after genetic studies had correlated LDL levels in some patients with
35
36 mutations associated with gain or loss of function of PCSK9;^{11,12} two loss of function mutations
37
38 correlate with significantly reduced risk of coronary heart disease.¹¹ Indeed, an individual with
39
40 no detectable PCSK9, and extremely low LDL levels, was healthy, suggesting suppression of
41
42 PCSK9 for lipid lowering is safe.¹³ Conversely, individuals with gain-of-function mutations in
43
44 PCSK9 have a higher risk of coronary heart disease.^{11,12}
45
46
47
48
49
50
51
52
53
54
55
56
57
58
59
60

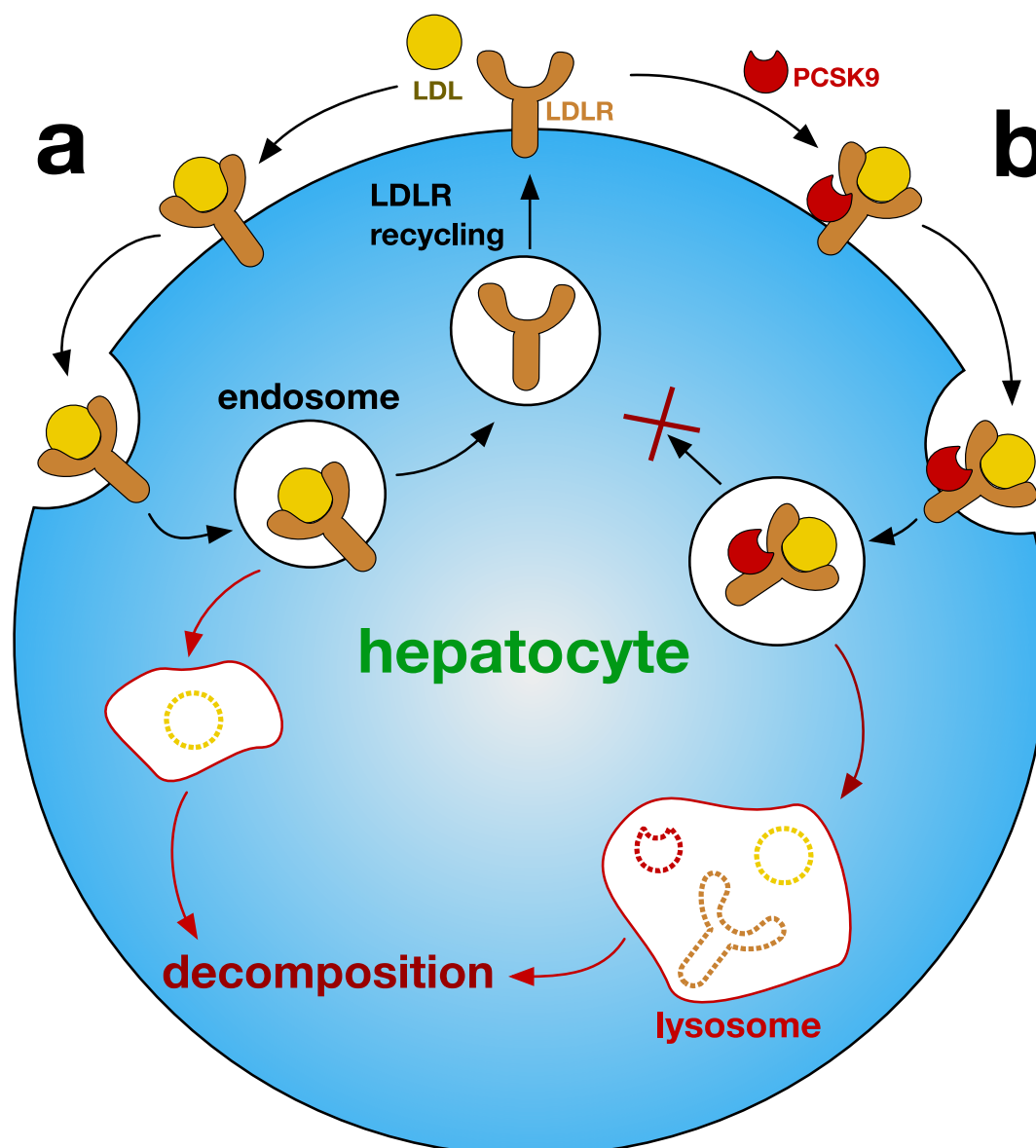
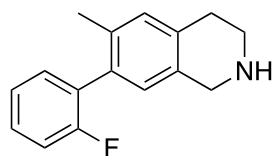


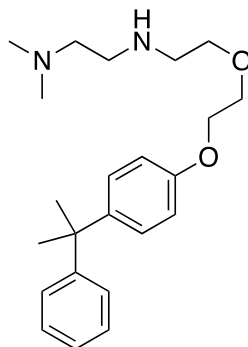
Figure 1. **a** In the absence of PCSK9, LDL•LDLR is endocytosed onto hepatocytes, then the LDLR is recycled and LDL is digested; and, **b** In the presence of PCSK9, LDLR is not recycled and the whole complex is decomposed. Thus PCSK9•LDLR interaction suppresses recycling of LDLR and diminishes uptake of LDL particles by the liver.

1 Multiple clinical studies have shown injectable antibody therapeutics that impede the
2 PCSK9•LDLR protein-protein interaction (PPI) significantly decrease circulating LDL levels.¹⁴
3
4 Subsequently, two antibody drugs that disrupt PCSK9•LDLR are FDA approved (Repatha from
5 Amgen and Praluent from Sanofi/Regeneron); they appear to be tolerated well, with no serious
6
7 side effects, and are efficacious.¹⁵⁻²⁰ PCSK9•LDLR therefore is a validated target for medicinal
8
9 chemistry.
10
11
12

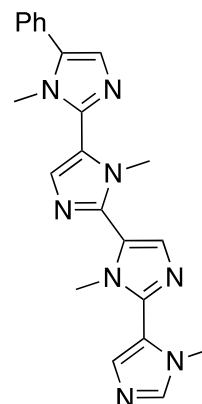
13
14 The preferred modality for disruption of PCSK9•LDLR, however, is small molecule drugs, not
15 mAbs, on the basis of mode of administration, cost, shelf life, and immunogenic response
16
17 issues. Thus in 2014 GenenTech stated: “Undoubtedly, an orally available small molecule
18
19 inhibitor of PCSK9, due to lower cost and ease of administration, would be a highly desirable
20
21 alternative therapeutic agent.”²¹ Peptides have been used to mimic either component in the
22
23 PCSK9•LDLR interaction²²⁻²⁸ but they have poor efficacy in plasma. There are limited reports
24
25 of non-peptidic small molecules that effectively inhibit the PCSK9•LDLR interaction, despite of
26
27 intense efforts to find such compounds. Portola Pharmaceuticals have reported
28
29 tetrahydroisoquinolines that increased LDL-uptake into liver cells, and LDLR cell surface
30
31 populations.²⁹ Similarly, Park *et al* reported compounds that had the same types of activities
32
33 *and* reduced LDL in wild type mice but not the corresponding a PCSK9 knock out murine
34
35 model.^{30,31} The Park compounds have fragments that structurally resemble the plasticizer
36
37 **BPA**. Both the Portola and Park studies do not report any direct evidence that these small
38
39 molecules bind PCSK9; the compounds could act via another mechanism. However, Stucchi
40
41 *et al* reported an oligo *N*-methyl imidazole that induced concentration dependent disruption of
42
43 PCSK9•LDLR based on an ELISA assay, and increased LDL uptake in HepG2 cells.
44
45 Curiously, the IC₅₀ reported for the binding of this compound to PCSK9 (11.2 ± 0.2 μM) was
46
47 *greater* than the EC₅₀ for increased LDL uptake into HepG2 cells (6.04 μM).
48
49
50
51
52
53
54
55
56
57
58
59
60



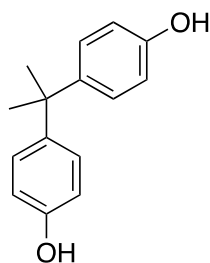
*Portola
Pharmaceuticals*



Park et al



Stucchi et al



BPA

Our labs have developed a technique for accelerated discovery of small molecules that inhibit PPIs: *EKO (Exploring Key Orientations)*.^{32,33} *EKO* features relatively rigid, usually non-peptidic, chemotypes with three amino acid side-chains. Preferred conformations of these chemotypes are simulated then systematically compared, via a data mining algorithm, with side-chain orientations of protein-protein interface amino acids in solid-state structures. A chemotype that overlays well on one protein at the interface is a candidate to displace that same protein from the PPI.

Research featured here illustrates how the *EKO* approach was used to discover small molecules that bind PCSK9 with low micromolar affinities, which prevent the PCSK9•LDLR interaction in LDL uptake by hepatocytes.

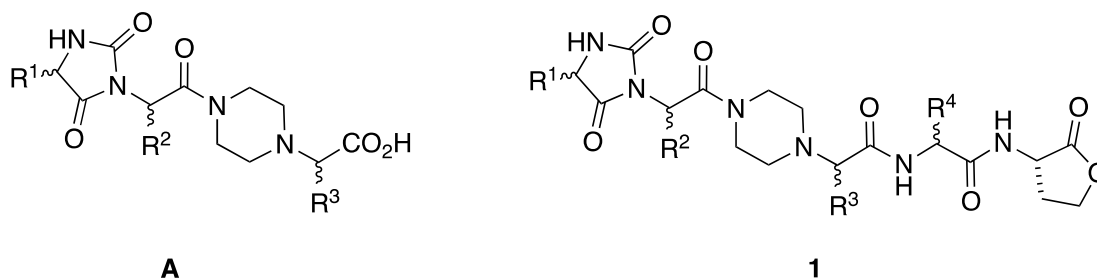
RESULTS AND DISCUSSION

Small Molecule Design And Syntheses

Several candidate chemotypes were conceived and screened using the EKO approach. In EKO, preferred conformations of the featured chemotypes with three methyl side-chains are simulated, but they may overlay on any three residues of a protein in a PPI. Chemotypes with side-chains corresponding to the protein at the overlay sites must then be prepared and assayed to test the validity of the EKO-prediction.

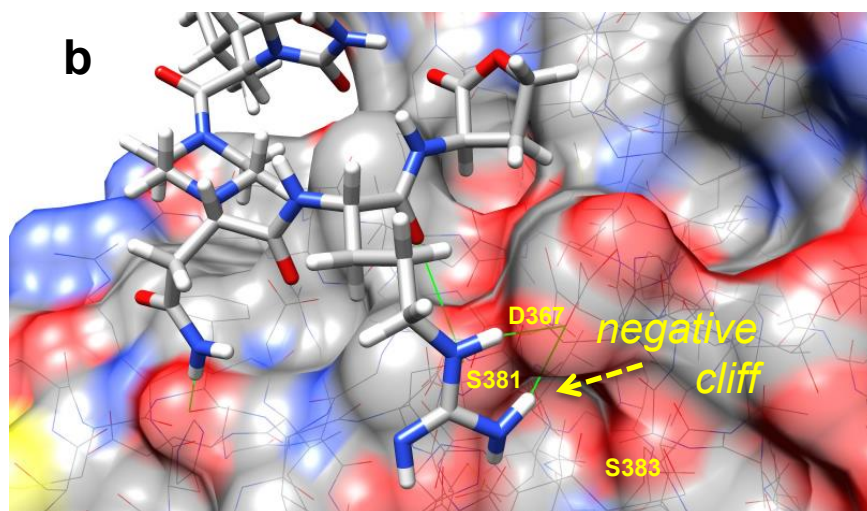
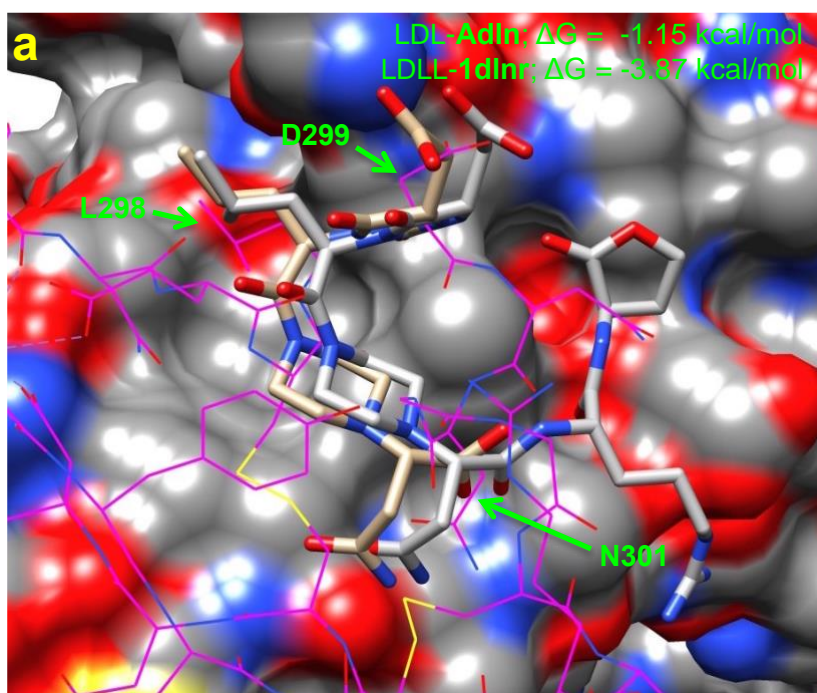
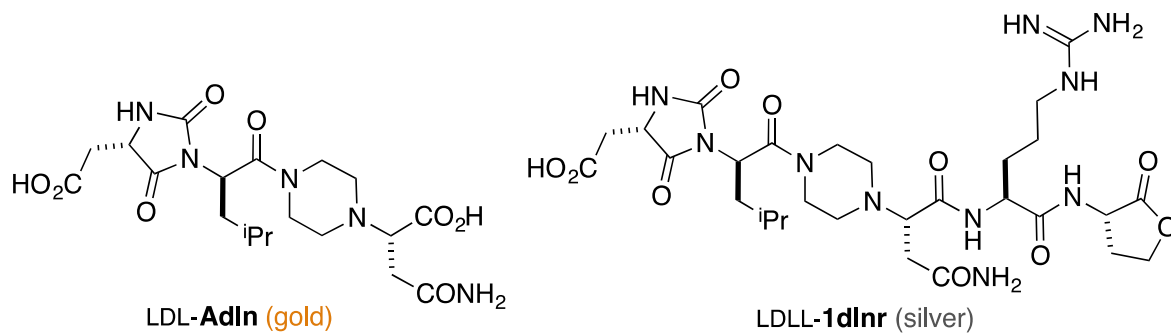
In the event, molecules in series **A** gave several overlays on LDLR of the PCSK9•LDLR complex (crystal structure PDB identifier 3gcx).³⁴ Specifically, EKO indicated preferred conformations of structures **A** overlaid C α – C β atoms well on the following sets of interface side-chains of LDLR in the PCSK9•LDLR crystal structure: Asp²⁹⁹, Leu²⁹⁸, Asp³⁰¹; Cys²⁹⁷, Asn³⁰¹, Asp²⁹⁹; Leu²⁹⁸, Asp²⁹⁹, Asn³⁰¹; Val³⁰⁷, Cys³⁰⁸, Leu³¹⁸; Asn³⁰⁹, Cys³⁰⁸, Leu³¹⁸. Thus the residues implicated in total were: Cys²⁹⁷, Leu²⁹⁸, Asp²⁹⁹, Asp³⁰¹, Val³⁰⁷, Cys³⁰⁸, Asn³⁰⁹, and Leu³¹⁸. Based on Ala-scan studies, Horton *et al* conclude the LDLR side-chains implicated in PCSK9•LDLR hot-spots are Asn²⁹⁵, Glu²⁹⁶, Asp³¹⁰, Tyr³¹⁵,⁸ while crystallographic evidence led others to suggest Asp²⁹⁹, Leu³¹⁸, and Asn³⁰⁹ were implicated.³⁵ Throughout we have underlined residues that have been postulated to be hot-spots that were also overlaid via preferred conformations of **A**. In our view, presence, or lack of, overlap with hot-spots is insufficient grounds for “go” or “no-go” decisions in EKO analyses. There are two reasons for this: (i) the uncertainties of predicting hot-spots³⁶ even with experimental data; and, (ii) the notion of isolated hot-spots is being superseded by *hot segments* in which disruption of one residue in a tightly packed arrangement alters the contributions of the others.³⁷⁻³⁹

Several compounds in series **A** were prepared and tested using a commercial TR-FRET assay (BPS Bioscience Inc., San Diego, CA); however, the results were inconclusive (Figure S1).



We were unsure if this negative result was because of poor affinity of the compounds **A**, insufficient sensitivity in the TR-FRET assay, or both. In any event, it seemed clear that modifications to improve the affinity of the core **A** towards PCSK9 would be desirable. Consequently, an iterative docking and energy minimization procedure was used to virtually modify chemotypes **A** to include additional pharmacophores that would increase binding efficiencies. Specifically, the preferred conformations of **A** were overlaid on LDLR in the 3gcx structure, LDLR was removed, then the chemotypes were docked in place using Glide within the Schrodinger package.⁴⁰⁻⁴² That procedure gave “baseline energies” for interactions of **A** with PCSK9 to which data from docking virtually modified analogs could be compared;⁴³ this procedure was performed in the Schrodinger software package using the CombiGlide routine.

Figure 2a shows a docked and minimized structure of **A**•PCSK9 generated from the original EKO overlay. We noticed that there is a conspicuous negatively charged cavity in PCSK9 comprising Ser383, Asp367 and Ser381 proximal to the C-terminus of **A**, but not interacting with it. Consequently, we made that cavity a priority in CombiGlide simulations. Those calculations indicated that negative pocket was filled by addition of His, Lys or, optimally, Arg at the **A** C-terminus; structures **1** were conceived in this way. Figure 2b illustrates how that Arg in the small molecule H-bonds to Asp³⁶⁷.



53
54
55
56
57
58
59

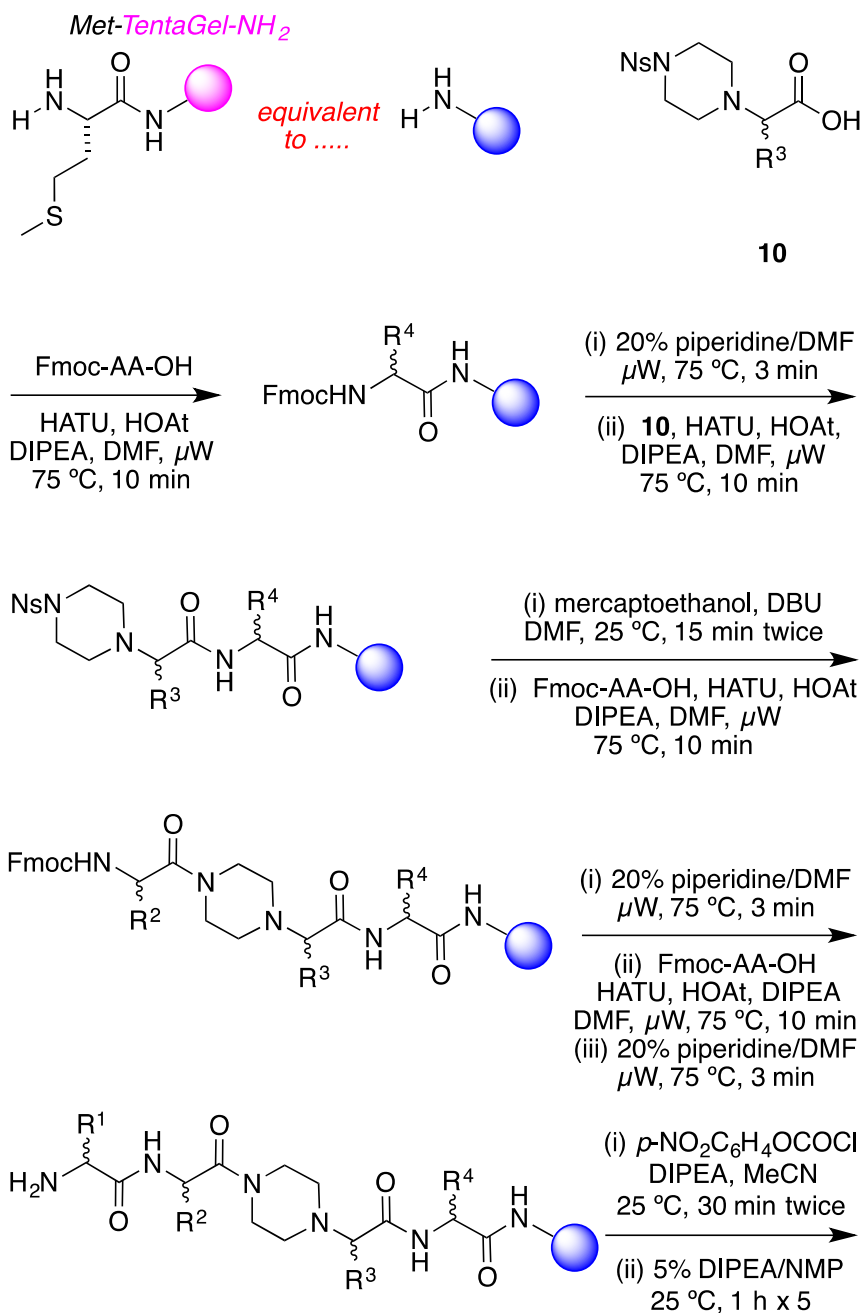
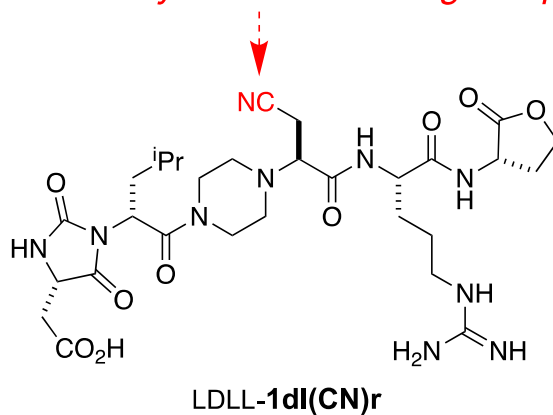
Figure 2. Docking of LDL-AdIn (gold) and LDLL-1dInr (silver) onto PCSK9. **a** Compounds LDL-AdIn and LDLL-1dInr overlay on the LDLR (shown in magenta wire), in which six $C\alpha$ - $C\beta$ atoms of chemotypes and LDLR side-chains (green arrows) are compared; RMSD = 1.75 and 1.95 Å for LDL-

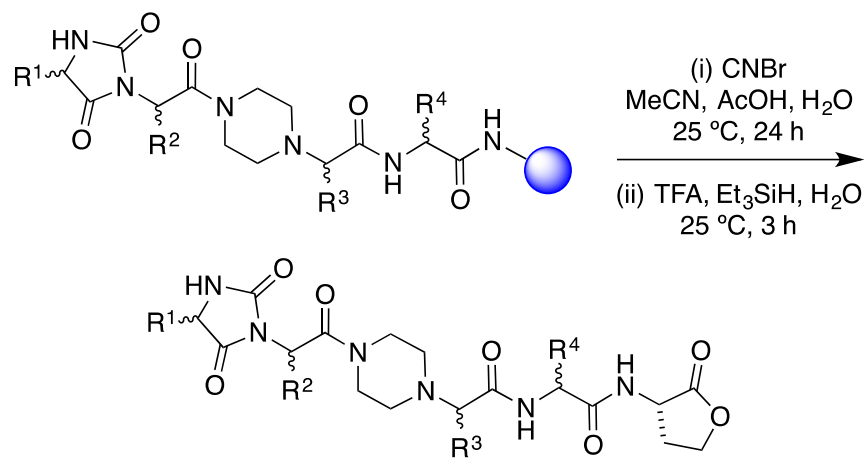
1 **Adln** and LDLL-**1dlnr**, respectively. **b** Improving binding affinity of LDLL-**1dlnr** is likely due to the H-
2 bonds of Arg residue to the Asp³⁶⁷ of PCSK9 at a negative “cliff face” region as indicated in green lines.
3
4
5
6
7

8 A solid phase synthesis of chemotypes **1** on TentaGel-NH₂ resin was developed (Scheme 1).
9
10 Microwave accelerated amino acid couplings installed the R⁴-bearing residue, then the
11 protected amino acid fragment **10** that carries R³. Nosyl-removal as indicated,⁴⁴ then two
12 more coupling-deprotection cycles using standard *N*-Fmoc-protected amino acids assembled
13 the fragments bearing the R² and R¹ side-chains. The Fmoc was removed, and the *N*-terminal
14 dipeptide was converted to a hydantoin via a two-step process.⁴⁵ Finally, cyanogen bromide
15 was used to cleave the protected chemotypes **1** from the resin, giving the *C*-terminal lactone
16 appendix in these structures.
17
18
19
20
21
22
23
24
25
26

27 Compounds in Scheme 1 and throughout this paper are numbered according to the scaffold
28 (or scaffold-intermediate). Lower case one-letter codes are used to delineate the amino acid
29 side-chains R¹ – R⁴ and relate them to the closest amino acid; primed letters indicate
30 protected side-chains (eg **d'** for the –CH₂CO₂^tBu of Asp and **k'** for the –(CH₂)₄NHBoc of Lys).
31
32
33
34
35
36

37 Implementation of Scheme 1 gave 15 compounds for screening, but one, LLLD-**1ldnq**, was
38 surprisingly vulnerable to degradation in the air, and was not considered further. One of the
39 compounds that was considered, LDLL-**1dl(CN)r**, is a byproduct formed via dehydration of the
40 Asn side-chain in the cyanogen bromide cleavage step.
41
42
43
44
45
46
47
48
49
50
51
52
53
54
55
56
57
58
59
60

amide dehydrated in cleavage step



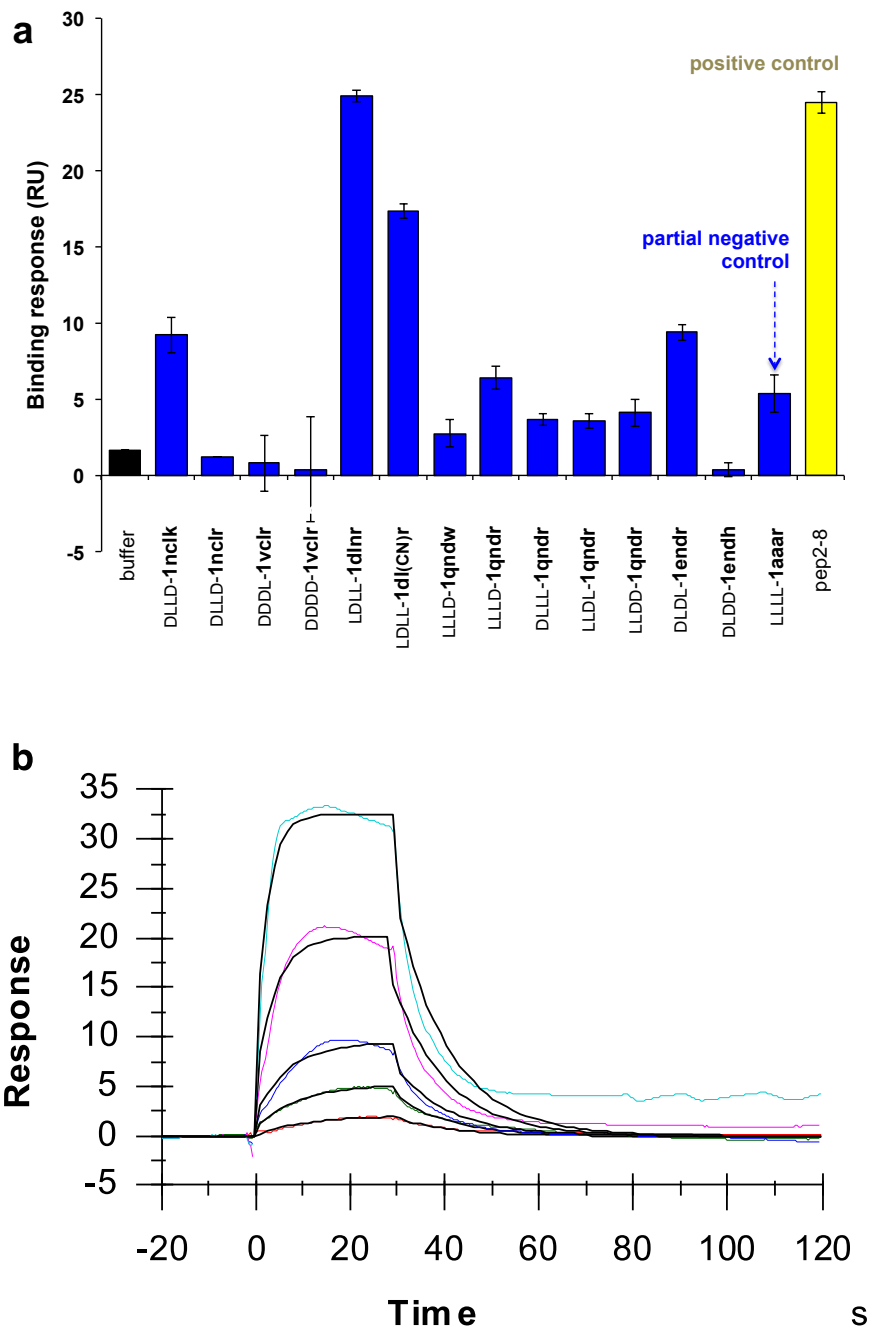
DLLD-1ncl_k; DLLD-1ncl_r; DDDL-1vcl_r
 DDDD-1vcl_r; LDLL-1dl_{nr}; LDLL-1dl(CN)_r
 LLLD-1qnd_w; LLLD-1qnd_r; DLLL-1qnd_r
 LLDL-1qnd_r; LLDD-1qnd_r; DLDL-1end_r
 DLDD-1end_h; LLLD-1ldn_q; LLLL-1aa_r

23 **Scheme 1.** Solid phase syntheses of chemotypes **1**.
 24
 25
 26
 27
 28
 29
 30
 31
 32
 33
 34
 35
 36
 37
 38
 39
 40
 41
 42
 43
 44
 45
 46
 47
 48
 49
 50
 51
 52
 53
 54
 55
 56
 57
 58
 59
 60

Binding Assays

Surface plasmon resonance (SPR) was used to screen the library of 14 compounds indicated in Figure 3a. Pep2-8 is a 13-residue peptide developed by GenenTech that was reported to bind PCSK9 ($K_d 0.66 \pm 0.11 \mu\text{M}$)²¹, and was used here as a positive control. Compound, LLLL-**1aaar**, is a “partial negative control” having the same core as the EKO-implicated compounds, but only Ala side-chains and an all-L stereochemistry that was not predicted via EKO, *ie* LLLL-**1aaar** controls for random stereochemistry and lack of functional side-chains. In the event, three compounds and Pep2-8 were selected (on the basis of this initial SPR data and the cellular uptake assays described below) for more thorough SPR analyses: LDLL-**1dlnr** ($K_d 24.8 \pm 9.1 \mu\text{M}$; Figure 3b), DLDD-**1nclk** ($41.2 \pm 17.5 \mu\text{M}$; Figure S7b), LDLL-**1dl(CN)r** ($35.8 \pm 11.4 \mu\text{M}$; Figure S7d), and Pep2-8 ($3.56 \pm 0.16 \mu\text{M}$). The K_d for Pep2-8 determined here is slightly higher than the value reported previously;²¹ this discrepancy might be because of different techniques used to study dissociation constant (the literature procedure used was biolayer interferometry).

Seven compounds in the library (again, selected on the basis of the SPR data and the cellular assays described below) were subjected to an ELISA assay to obtain additional evidence that the small molecules bind PCSK9 (Figure 3c). Error limits in this assay are higher than in the SPR experiments. All the compounds tested showed increased inhibition of PCSK9 to the EGF-AB domain of LDLR relative to a blank control. Inhibition by the compounds in this assay was one to two orders of magnitude less than the positive control pep2-8.



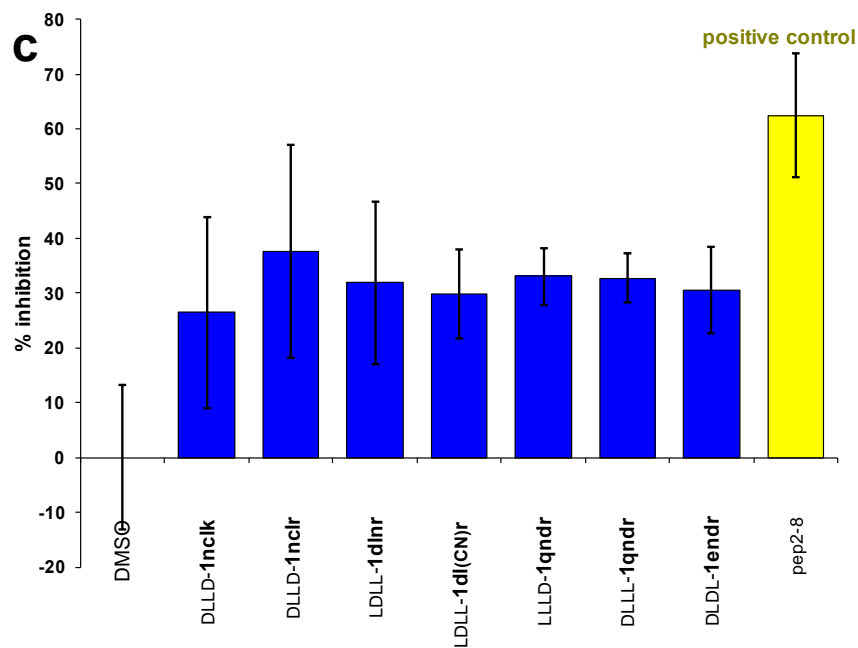
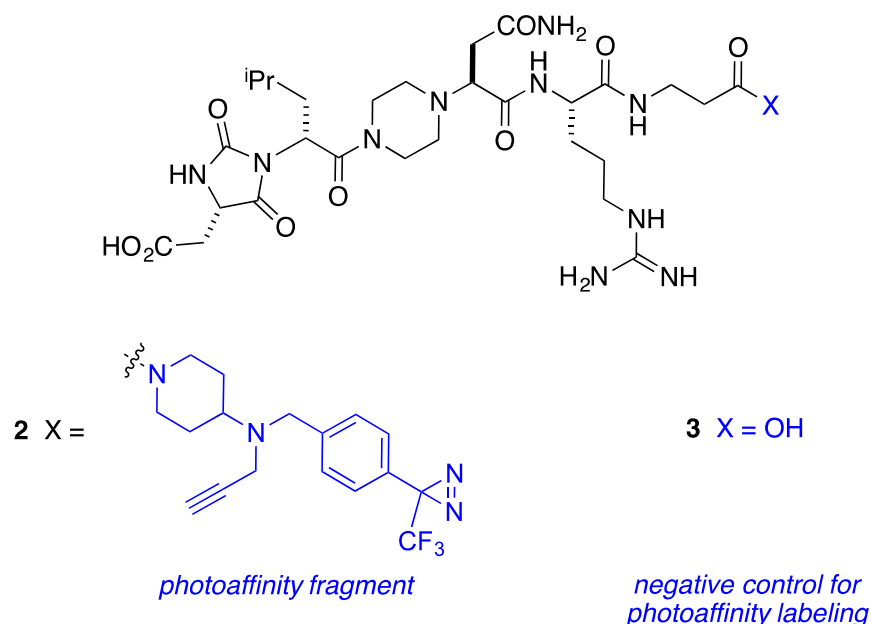


Figure 3. **a** Initial SPR screening of 14 compounds at 50 μM and pep2-8 at 5 μM over PCSK9 supported on gold via amine coupling chemistry. **b** Sensorgram of LDLL-1dlR within 1-54 μM concentration range showing the estimated K_d was 24.8 ± 9.1 μM ($k_{on} = (4.04 \pm 2.20) \times 10^3$ M⁻¹s⁻¹, $k_{off} = (8.74 \pm 3.40) \times 10^{-2}$ s⁻¹). **c** Selected compounds and pep2-8 were screened at 50 μM for inhibitory effect against 50 ng/mL of PCSK9 using PCSK9-LDLR *in vitro* binding assay kit (MBLI Co., MA) following the manufacture instructions. Results are the averages ± SD of three independent experiments

Photoaffinity Labeling

Two derivatives of LDLL-**1dlnr**, compounds **2** and **3**, were prepared to explore if binding of these to PCSK9 could be detected via photoaffinity labeling. Thus, a protected fragment of LDLL-**1dlnr** was prepared on chlorotrityl resin, cleaved with the protecting groups in place, and coupled to a photoaffinity fragment designed in these laboratories (see supporting).



Pre-incubation of PCSK9 with **2** and (optionally) with a large excess of the blocking ligand **3**, irradiation of some wells at 365 nm, copper-mediated click reaction with Alexa-488-azide, then SDS-PAGE gave the data shown in Figure 4. A fluorescent band corresponding to the molecular mass of labeled PCSK9 (~60 kDa) was observed only in the wells that were irradiated in the absence of the blocking ligand **3**.

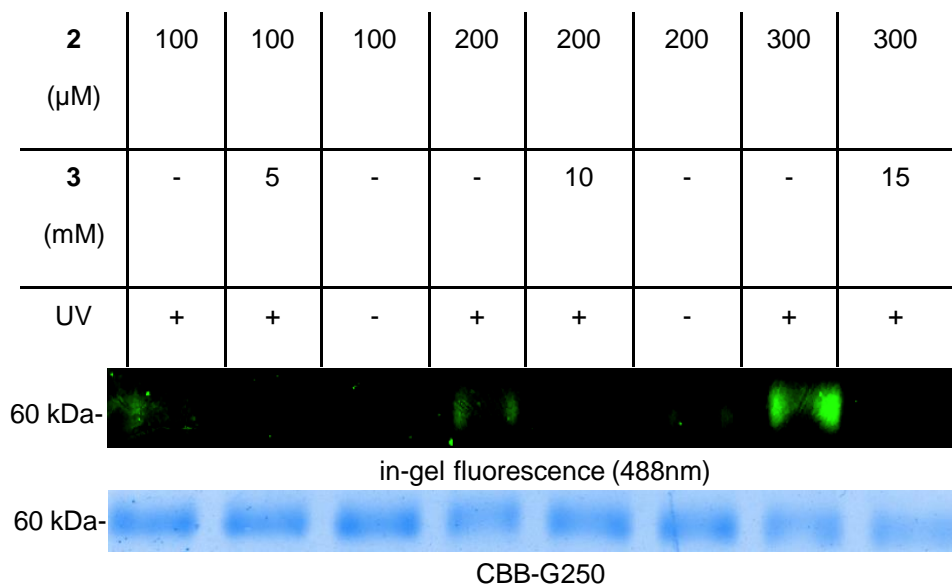


Figure 4. Photoaffinity labeling of human PCSK9 protein with **2**. PCSK9 was incubated with PAL ligand **2**, and optionally pretreated with 50-fold excess of the competition ligand **3**. UV (365 nm) irradiation, then Cu-mediated click with Alexa-488-azide gave the samples for analysis. These samples were diluted in SDS sample buffer and subjected to SDS-PAGE. Fluorescent proteins were detected by in-gel fluorescence (Alexa 488) and all proteins were stained with CBB (Coomassie Brilliant Blue) G250.

Liver-cell Uptake Assays

1
2
3 The seven select compounds shown in Figure 3c were tested for cytotoxicity using liver cells
4 (hepatocytes; HepG2). All seven of these compounds showed no toxicity up to 50 μ M. The
5
6 compound with the lowest K_d in SPR studies, LDLL-**1dlnr**, was also checked at 100 μ M and
7
8 showed no cytotoxicity even at these higher concentration (Figure S2). In another prelude to
9
10 the key cellular assays, the water solubilities of the featured compounds were measured. The
11
12 solubility concentration gradients for these materials were linear to beyond 100 μ M, *ie* they
13
14 were soluble at the maximum concentration used in the uptake assays below (Figure S5).
15
16 Compounds **A** and **1** were evaluated their drug likeliness by QikProp calculations^{46,47} to
17
18 determine absorption, distribution, metabolism and excretion (ADME) properties, and the
19
20 results are reported in the supporting material (Table S3 and S4).
21
22
23
24
25
26

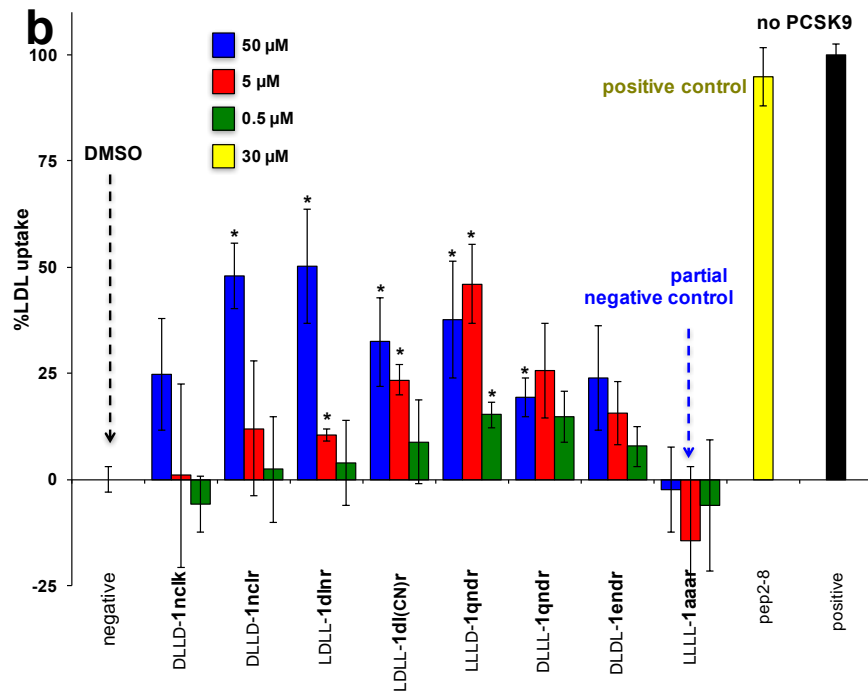
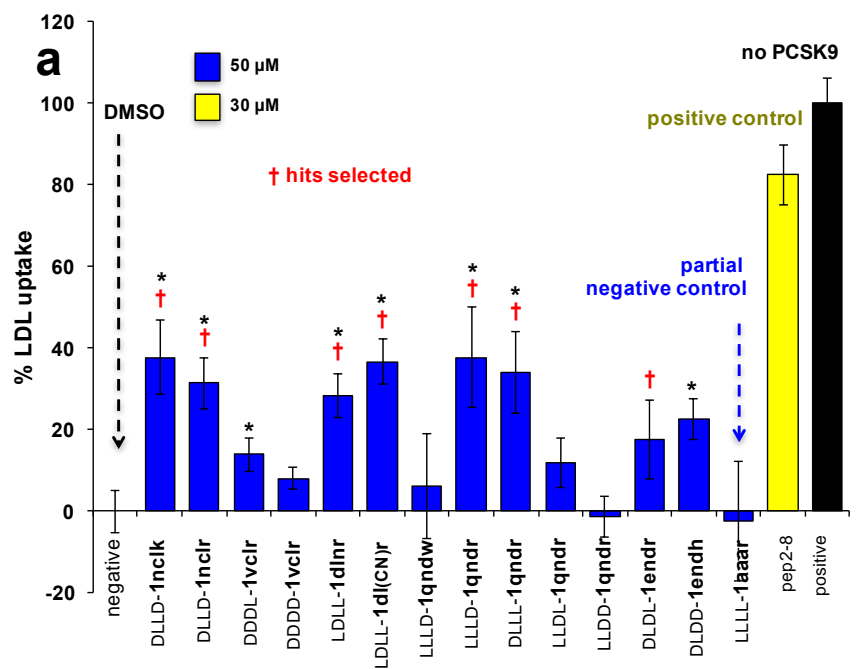
27 An established assay for PCSK9•LDLR inhibition features uptake of fluorescently labeled LDL
28
29 nanoparticles (BODIPY-LDL, Invitrogen) by hepatocytes; the cells become fluorescent as the
30
31 particles are absorbed.²¹ Uptake of the BODIPY-containing particles is maximized in the
32
33 absence of PCSK9, and the cells become fluorescent; conversely, adding PCSK9 diminishes
34
35 that signal. Addition of PCSK9 *and* a compound that interferes with the PCSK9•LDLR
36
37 interaction would be expected to give cells that are more fluorescent than those to which only
38
39 PCSK9 was added but less so than cells to which none of that protein was present.
40
41
42
43

44 Figure 5a shows maximal uptake (calibrated to 100 %; black bar) in the absence of PCSK9,
45
46 while all the other data points correspond to 15 μ g/mL of that protein; the “negative”
47
48 corresponds to only PCSK9 added (calibrated to 0 %). Pep2-8 at 30 μ M restored the LDL
49
50 uptake (yellow bar) to within 80 % of its maximal value (black). Several of the featured
51
52 chemotypes **1** showed promise insofar as they, like pep2-8, also restored fluorescence; the
53
54 ones marked with a red dagger were selected for further assays on the basis of this data and
55
56 the binding studies above. Recall that LLLL-**1aaar** is a “partial control” as described above
57
58
59
60

1 (same chemotype, just methyl side-chains, and random stereochemistry); it did *not* induce
2 significant BODIPY-LDL uptake.
3

4
5 Figure 5b shows data derived from repetition of these experiments under identical conditions
6 except that three different doses of the test compounds were used. Overall, all the
7
8 compounds show a dose response, except LLLD-**1qndr**, DLLL-**1qndr**, and, as expected, the
9
10 partial control LLLL-**1aar**. Figure 5c shows a more extensive dose-response curve for one
11
12 these compounds, LDLL-**1dlnr** (again, selected on the basis of the overall data); this data
13
14 shows an encouraging correspondence.
15
16
17
18

19
20 It is curious that LDL uptake in the HepG2 cells was significantly enhanced when 100 μ M of
21
22 compound was used (Fig 5c). This is consistent with the SPR binding data in which LDLL-
23
24 **1dlnr** showed a longer resident time (15-20 fold slower off-rate) compared with Pep2-8. More
25
26 particularly, the longer half-life of the LDLL-**1dlnr** • PCSK9 complex became more obvious
27
28 when higher concentration (100 μ M) of compound was injected onto the PCSK9-functionalized
29
30 surface (data not shown). One explanation for these observations is that there could be a
31
32 synergistic target site for LDLL-**1dlnr** that only becomes significant at higher compound
33
34 concentrations.
35
36
37
38
39
40
41
42
43
44
45
46
47
48
49
50
51
52
53
54
55
56
57
58
59
60



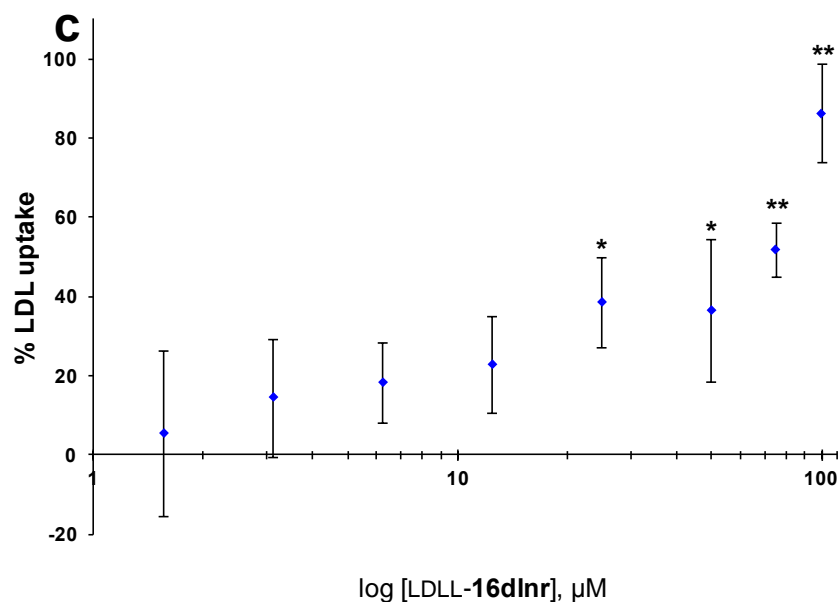
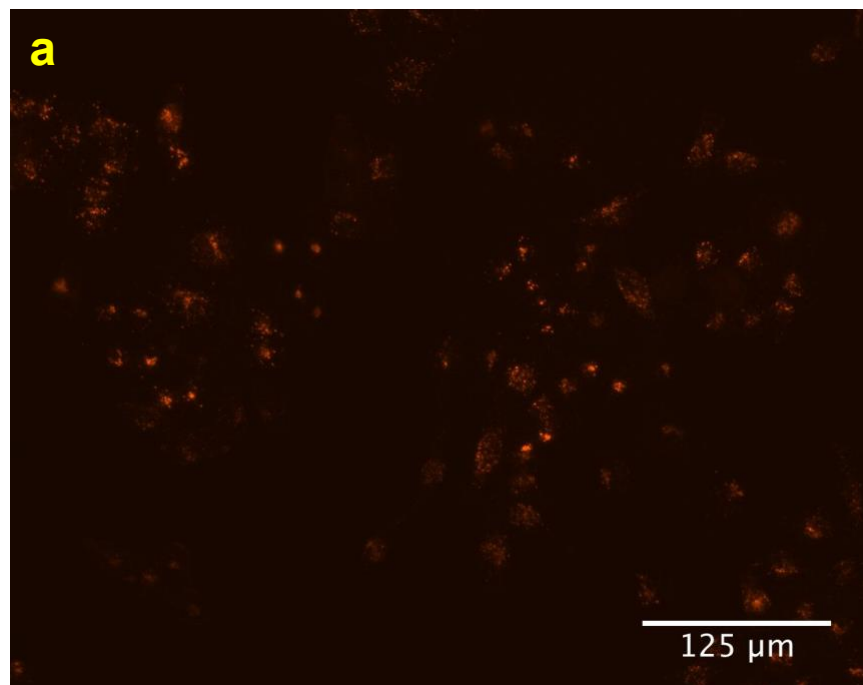


Figure 5. Uptake of BODIPY-LDL by hepatocytes. **a** Initial screen at 50 μM concentrations of the featured compounds. **b** Data of select compounds at three different doses. **c** A more extensive dose-response curve of one select lead: LDLL-1dlnr. All results are represented as means \pm SD of three independent experiments. Significant differences between compounds and negative control are determined using student' t-test (* $p \leq 0.05$, ** $p \leq 0.01$).

Cell-surface LDLR Assay

Two assays were attempted to probe if increased uptake of LDL particles correlates with increased expression of LDLR. Our initial attempts to do this featured monitoring LDLR levels on treated and untreated hepatocytes using flow cytometry. The data obtained (Figure S3) indicated an increase in LDLR levels upon treatment with the seven hit compounds (as shown in Figure 5b), but the errors in the measurements were such that the increases had borderline statistical significance. Consequently, we resorted to a semi-quantitative approach in which the LDLRs on live hepatocytes (treated and untreated) were visualized using an LDLR-

1 selective mAb in combination with an Alexa Fluor®-labeled secondary mAb. Figure 6a shows
2 expression of LDLR in the cells was suppressed when they were treated with PCSK9 alone.
3
4
5 When cells were treated with the test compound LDLL-1dlnr then they stained more brightly
6
7 (Figure 6b) though not as brilliant as the positive control culture that lacked PCSK9 and any
8
9 test compound (Figure 6c). Similar data including bright-field and merged images was
10
11 collected for another three of the featured compounds (see Supporting Figure S4).
12
13
14



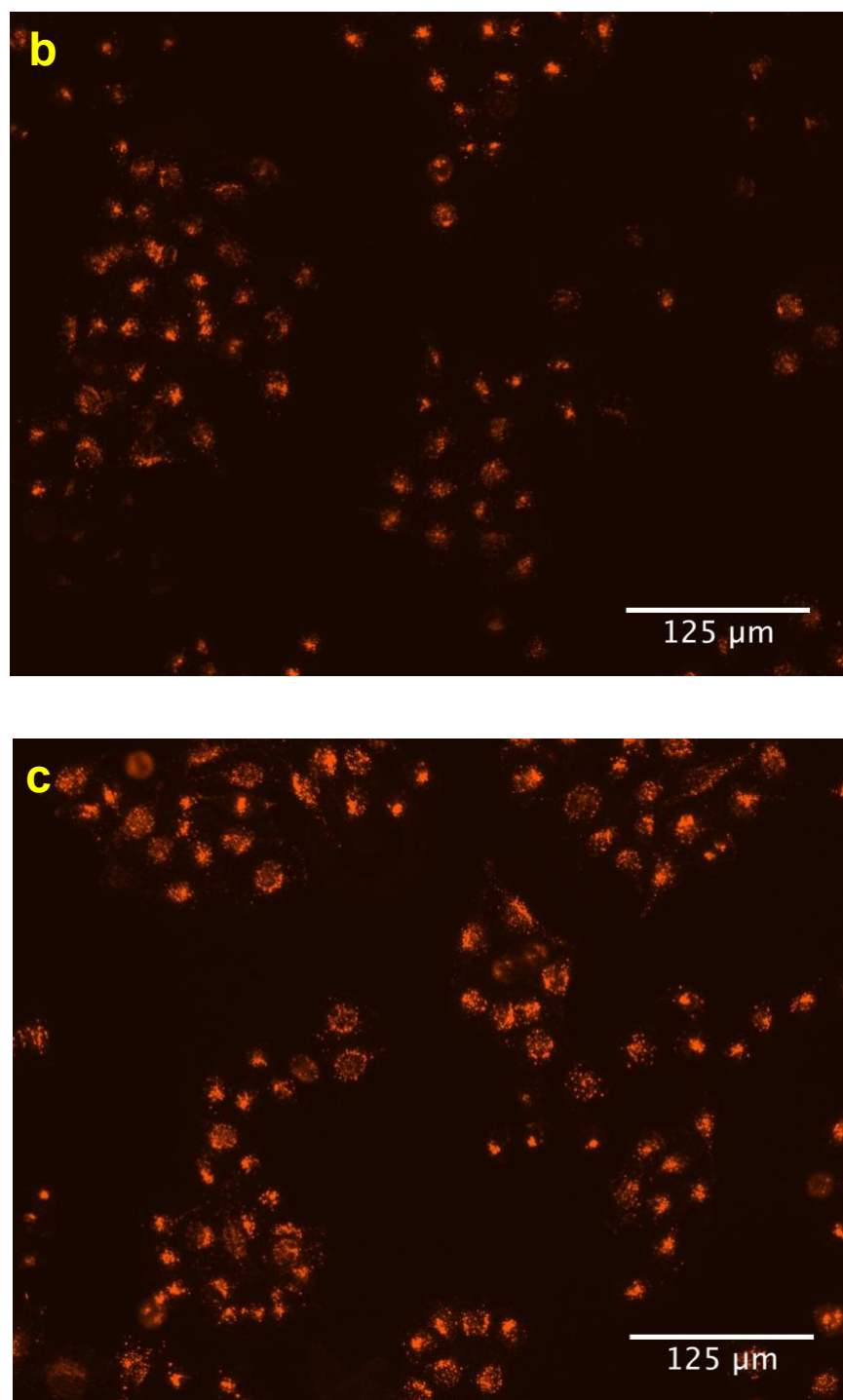


Figure 6. Cell-surface LDLRs of hepatocytes were determined by fluorescent imaging. HepG2 cells were treated (a) with PCSK9 alone (negative control); (b) with PCSK9 and LDLL-1dlNr; and (c) without PCSK9 (positive control).

CONCLUSION

1
2
3 This study was undertaken to find validated, small molecule leads that disrupt PCSK9•LDLR.
4
5 Structural modifications to chemotypes **1** are now planned to discover derivatives that retain
6
7 and improve on their encouraging binding and increased LDL uptake characteristics, while
8
9 simultaneously engineering in features to endow more favorable ADME properties. Thus, the
10
11 next steps in the process will probably involve substitution of amino acid side-chains with
12
13 bioisosteres to improve bioavailability,⁴⁸ and perhaps targeting the liver, eg via attaching
14
15 ligands implicated in galactose uptake.⁴⁹⁻⁵⁴
16
17
18

19
20 The chemical design component of this study involved conception of possible chemotypes,
21
22 implementation of the EKO approach, and one cycle of virtual pharmacophore screening.
23
24 Based on the two binding and three cellular assay presented, over half of the 13 test
25
26 compounds showed significant, measurable activities. Thus, the strategy brought a degree of
27
28 rationality to this process that led to a hit rate (~50%) that would be highly unlikely via high
29
30 throughput screening of random compounds against the same target. Moreover, the limitation
31
32 of EKO that requires the chemotypes considered must bear three amino acid side-chains is
33
34 also a strength insofar as it forces practitioners to explore virgin patent diversity space.
35
36
37
38
39
40
41
42
43
44
45
46
47
48
49
50
51
52
53
54
55
56
57
58
59
60

ASSOCIATED CONTENT

Supporting Information

Details of the solid phase syntheses, characterization of compounds **A** and **1 – 3**, protocols for the biological assays (LDL uptake, binding via SPR/ELISA/TR-FRET, MTT cell viability, and determination of relative levels of LDLR expression), determination of water solubilities, photoaffinity labeling, computational procedures, and predicted physiochemical characteristics.

This material is available free of charge via the internet at <http://pubs.acs.org>.

AUTHOR INFORMATION

Corresponding Author

burgess@tamu.edu

Notes

The authors declare no competing financial interests.

ACKNOWLEDGEMENTS

We thank Dr John Kulp of Small Molecule PPI Mimics LLC for useful discussions, Mr Jiang Zhengyang for help with the flow cytometry experiments, and Dr Jay Horton of UT Southwestern for the gift of the PCSK9 protein used in these studies. We thank DoD BCRP Breakthrough Award (BC141561), CPRIT (RP150559 and RP170144), The Robert A. Welch Foundation (A-1121). The NMR instrumentation at Texas A&M University was supported by a grant from the National Science Foundation (DBI-9970232) and the Texas A&M University System. The SPR studies were conducted in the protein interaction core at the Institute of Biosciences and Technology, TAMU, Houston, TX.

References

- 1
- 2
- 3
- 4 (1) Costet, P.; Krempf, M.; Cariou, B. *Trends Biochem. Sci.* **2008**, *33*, 426-434.
- 5 (2) Li, J.; Tumanut, C.; Gavigan, J.-A.; Huang, W.-J.; Hampton, E. N.; Tumanut, R.; Suen, K. F.;
6 Trauger, J. W.; Spraggon, G.; Lesley, S. A.; Liau, G.; Yowe, D.; Harris, J. L. *Biochem. J.* **2007**,
7 *406*, 203-207.
- 8 (3) McNutt, M. C.; Lagace, T. A.; Horton, J. D. *J. Biol. Chem.* **2007**, *282*, 20799-20803.
- 9 (4) Norata G., D.; Tibolla, G.; Catapano A., L. *Ann. Rev. Pharmacol. Toxicol.* **2014**, *54*, 273-293.
- 10 (5) Tveten, K.; Holla, O. L.; Cameron, J.; Strom, T. B.; Berge, K. E.; Laerdahl, J. K.; Leren, T. P.
11 *Hum. Mol. Genet.* **2012**, *21*, 1402-1409.
- 12 (6) Yamamoto, T.; Lu, C.; Ryan, R. O. *J. Biol. Chem.* **2011**, *286*, 5464-5470.
- 13 (7) Holla, O. L.; Cameron, J.; Tveten, K.; Stroem, T. B.; Berge, K. E.; Laerdahl, J. K.; Leren, T. P. *J.*
14 *Lipid Res.* **2011**, *52*, 1787-1794.
- 15 (8) Zhang, D.-W.; Lagace, T. A.; Garuti, R.; Zhao, Z.; McDonald, M.; Horton, J. D.; Cohen, J. C.;
16 Hobbs, H. H. *J. Biol. Chem.* **2007**, *282*, 18602-18612.
- 17 (9) Horton, J. D.; Cohen, J. C.; Hobbs, H. H. *J. Lipid Res.* **2009**, S172-S177.
- 18 (10) Seidah, N. G. *Expert Opin. Ther. Targets* **2009**, *13*, 19-28.
- 19 (11) Cohen, J. C.; Boerwinkle, E.; Mosley, T. H., Jr.; Hobbs, H. H. *N. Engl. J. Med.* **2006**, *354*, 1264-
20 1272.
- 21 (12) Abifadel, M.; Varret, M.; Rabes, J.-P.; Allard, D.; Ouguerram, K.; Devillers, M.; Cruaud, C.;
22 Benjannet, S.; Wickham, L.; Erlich, D.; Derre, A.; Villeger, L.; Farnier, M.; Beucler, I.; Bruckert,
23 E.; Chambaz, J.; Chanu, B.; Lecerf, J.-M.; Luc, G.; Moulin, P.; Weissenbach, J.; Prat, A.;
24 Krempf, M.; Junien, C.; Seidah, N. G.; Boileau, C. *Nat. Genet.* **2003**, *34*, 154-156.
- 25 (13) Zhao, Z.; Tuakli-Wosornu, Y.; Lagace, T. A.; Kinch, L.; Grishin, N. V.; Horton, J. D.; Cohen, J.
26 C.; Hobbs, H. H. *Am. J. Hum. Genet.* **2006**, *79*, 514-523.
- 27 (14) Steinberg, D.; Witztum, J. L. *Proc. Natl. Acad. Sci.* **2009**, *106*, 9546-9547.
- 28 (15) Stein, E. A.; Swergold, G. D. *Curr. Atheroscler. Rep.* **2013**, *15*, 1-14.
- 29 (16) Seidah, N. G.; Prat, A. *Nat. Rev. Drug Discovery* **2012**, *11*, 367-383.
- 30 (17) Chan, J. C. Y.; Piper, D. E.; Cao, Q.; Liu, D.; King, C.; Wang, W.; Tang, J.; Liu, Q.; Higbee, J.;
31 Xia, Z.; Di, Y.; Shetterly, S.; Arimura, Z.; Salomonis, H.; Romanow, W. G.; Thibault, S. T.;
32 Zhang, R.; Cao, P.; Yang, X.-P.; Yu, T.; Lu, M.; Retter, M. W.; Kwon, G.; Henne, K.; Pan, O.;
33 Tsai, M.-M.; Fuchslocher, B.; Yang, E.; Zhou, L.; Lee, K. J.; Daris, M.; Sheng, J.; Wang, Y.;
34 Shen, W. D.; Yeh, W.-C.; Emery, M.; Walker, N. P. C.; Shan, B.; Schwarz, M.; Jackson, S. M.
35 *Proc. Natl. Acad. Sci.* **2009**, *106*, 9820-9825.
- 36 (18) Ni Yan, G.; Di Marco, S.; Condra Jon, H.; Peterson Laurence, B.; Wang, W.; Wang, F.; Pandit,
37 S.; Hammond Holly, A.; Rosa, R.; Cummings Richard, T.; Wood Dana, D.; Liu, X.; Bottomley
38 Matthew, J.; Shen, X.; Cubbon Rose, M.; Wang, S.-p.; Johns Douglas, G.; Volpari, C.; Hamuro,
39 L.; Chin, J.; Huang, L.; Zhao Jing, Z.; Vitelli, S.; Haytko, P.; Wisniewski, D.; Mitnaul Lyndon, J.;
40 Sparrow Carl, P.; Hubbard, B.; Carfi, A.; Sittlani, A. *J Lipid Res* **2011**, *52*, 78-86.
- 41 (19) Raal, F. J.; Stein, E. A.; Dufour, R.; Turner, T.; Civeira, F.; Burgess, L.; Langslet, G.; Scott, R.;
42 Olsson, A. G.; Sullivan, D.; Hovingh, G. K.; Cariou, B.; Gouni-Berthold, I.; Somaratne, R.;
43 Bridges, I.; Scott, R.; Wasserman, S. M.; Gaudet, D. *Lancet* **2015**, *385*, 331-340.
- 44 (20) Raal, F. J.; Honarpour, N.; Blom, D. J.; Hovingh, G. K.; Xu, F.; Scott, R.; Wasserman, S. M.;
45 Stein, E. A. *Lancet* **2015**, *385*, 341-350.
- 46 (21) Zhang, Y.; Eigenbrot, C.; Zhou, L.; Shia, S.; Li, W.; Quan, C.; Tom, J.; Moran, P.; Di Lello, P.;
47 Skelton, N. J.; Kong-Beltran, M.; Peterson, A.; Kirchhofer, D. *J. Biol. Chem.* **2014**, *289*, 942-955.
- 48 (22) Mayer, G.; Poirier, S.; Seidah, N. G. *J. Biol. Chem.* **2008**, *283*, 31791-31801.
- 49 (23) Seidah, N. G.; Poirier, S.; Denis, M.; Parker, R.; Miao, B.; Mapelli, C.; Prat, A.; Wassef, H.;
50 Davignon, J.; Hajjar, K. A.; Mayer, G. *PLoS One* **2012**, *7*, e41865.
- 51 (24) Shan, L.; Pang, L.; Zhang, R.; Murgolo, N. J.; Lan, H.; Hedrick, J. A. *Biochem. Biophys. Res.*
52 *Commun.* **2008**, *375*, 69-73.
- 53 (25) Du, F.; Hui, Y.; Zhang, M.; Linton, M. F.; Fazio, S.; Fan, D. *J. Biol. Chem.* **2011**, *286*, 43054-
54 43061.
- 55 (26) Palmer-Smith, H.; Basak, A. *Curr. Med. Chem.* **2010**, *17*, 2168-2182.
- 56 (27) Lammi, C.; Zannoni, C.; Aiello, G.; Arnoldi, A.; Grazioso, G. *Sci. Rep.* **2016**, *6*, 29931.
- 57
- 58
- 59
- 60

- 1 (28) Guay, D.; Crane, S.; Lachance, N.; Chiasson, J.-F.; Truong, V. L.; Lacombe, P.; Skorey, K.;
2 Seidah, N. G. *WO 2014139008*, 2014.
- 3 (29) Barta, T. E.; Bourne, J. W.; Monroe, K. D.; Muehlemann, M. M.; Pandey, A.; Bowers, S.
4 *WO 2017034990*, 2017.
- 5 (30) Min, D.-K.; Lee, H.-S.; Lee, N.; Lee, C. J.; Song, H. J.; Yang, G. E.; Yoon, D.; Park, S. W.
6 *Yonsei Med. J.* **2015**, *56*, 1251-1257.
- 7 (31) Park, S. W.; Lee, H. S.; Min, D. K.; Lee, N. R.; Lee, C. J.; Yang, G. E. *WO 2016108572*, 2016.
- 8 (32) Ko, E.; Raghuraman, A.; Perez, L. M.; Ioerger, T. R.; Burgess, K. *J. Am. Chem. Soc.* **2013**, *135*,
9 167-173.
- 10 (33) Xin, D.; Holzenburg, A.; Burgess, K. *Chem. Sci.* **2014**, *5*, 4914-4921.
- 11 (34) McNutt, M. C.; Kwon, H. J.; Chen, C.; Chen, J. R.; Horton, J. D.; Lagace, T. A. *J. Biol. Chem.*
12 **2009**, *284*, 10561-10570.
- 13 (35) Kwon, H. J.; Lagace, T. A.; McNutt, M. C.; Horton, J. D.; Deisenhofer, J. *Proc. Natl. Acad. Sci.*
14 **2008**, *105*, 1820-1825.
- 15 (36) Kortemme, T.; Kim David, E.; Baker, D. *Sci STKE* **2004**, *2004*, pl2.
- 16 (37) Koes, D. R.; Camacho, C. J. *Bioinformatics* **2012**, *28*, 784-791.
- 17 (38) Accordino, S. R.; Morini, M. A.; Sierra, M. B.; Fris, J. A. R.; Appignanesi, G. A.; Fernandez, A.
18 *Proteins Struct. Funct. Bioinf.* **2012**, *80*, 1755-1765.
- 19 (39) London, N.; Raveh, B.; Schueler-Furman, O. *Curr. Opin. Chem. Biol.* **2013**, *17*, 952-959.
- 20 (40) Friesner, R. A.; Banks, J. L.; Murphy, R. B.; Halgren, T. A.; Klicic, J. J.; Mainz, D. T.; Repasky,
21 M. P.; Knoll, E. H.; Shelley, M.; Perry, J. K.; Shaw, D. E.; Francis, P.; Shenkin, P. S. *J. Med.*
22 *Chem.* **2004**, *47*, 1739-1749.
- 23 (41) Halgren, T. A.; Murphy, R. B.; Friesner, R. A.; Beard, H. S.; Frye, L. L.; Pollard, W. T.; Banks, J.
24 *J. Med. Chem.* **2004**, *47*, 1750-1759.
- 25 (42) Friesner, R. A.; Murphy, R. B.; Repasky, M. P.; Frye, L. L.; Greenwood, J. R.; Halgren, T. A.;
26 Sanschagrín, P. C.; Mainz, D. T. *J. Med. Chem.* **2006**, *49*, 6177-6196.
- 27 (43) Kaminski, G. A.; Friesner, R. A.; Tirado-Rives, J.; Jorgensen, W. L. *J. Phys. Chem. B* **2001**,
28 *105*, 6474-6487.
- 29 (44) Kan, T.; Fukuyama, T. *Chem. Commun.* **2004**, 353-359.
- 30 (45) Meusel, M.; Guetschow, M. *Org. Prep. Proced. Int.* **2004**, *36*, 391-443.
- 31 (46) Jorgensen, W. L.; Duffy, E. M. *Bioorg. Med. Chem. Lett.* **2000**, *10*, 1155-1158.
- 32 (47) Duffy, E. M.; Jorgensen, W. L. *J. Am. Chem. Soc.* **2000**, *122*, 2878-2888.
- 33 (48) Wipf, P.; Xiao, J.; Stephenson, C. R. J. *Chimia* **2009**, *63*, 764-775.
- 34 (49) Lee, M. H.; Han, J. H.; Kwon, P.-S.; Bhuniya, S.; Kim, J. Y.; Sessler, J. L.; Kang, C.; Kim, J. S.
35 *J. Am. Chem. Soc.* **2012**, *134*, 1316-1322.
- 36 (50) Thao, L. Q.; Lee, C.; Kim, B.; Lee, S.; Kim, T. H.; Kim, J. O.; Lee, E. S.; Oh, K. T.; Choi, H.-G.;
37 Yoo, S. D.; Youn, Y. S. *Colloids Surf., B* **2017**, *152*, 183-191.
- 38 (51) Lai, C.-H.; Chang, T.-C.; Chuang, Y.-J.; Tzou, D.-L.; Lin, C.-C. *Bioconjugate Chem.* **2013**, *24*,
39 1698-1709.
- 40 (52) Margarida Cardoso, M.; Peca, I. N.; Raposo, C. D.; Petrova, K. T.; Teresa Barros, M.; Gardner,
41 R.; Bicho, A. *J. Microencapsulation* **2016**, *33*, 315-322.
- 42 (53) Gankhuyag, N.; Singh, B.; Maharjan, S.; Choi, Y.-J.; Cho, C.-S.; Cho, M.-H. *Macromol. Biosci.*
43 **2015**, *15*, 777-787.
- 44 (54) Feng, L.; Yu, H.; Liu, Y.; Hu, X.; Li, J.; Xie, A.; Zhang, J.; Dong, W. *Polym. Chem.* **2014**, *5*,
45 7121-7130.
- 46
47
48
49
50
51
52
53
54
55
56
57
58
59

GRAPHICAL

